NASA TECHNICAL NOTE

NASA TN D-5750

c.1

NASA TN D-5750

DRAG CHARACTERISTICS OF SEVERAL TOWED DECELERATOR MODELS AT MACH 3

by Robert Miserentino and Herman L. Bohon

Langley Research Center
Hampton, Va. 23365

NATIONAL AERONAUTICS AND SPACE ADMINISTRATION • WASHINGTON, D. C. • MAY 1970

1. Report No. NASA TN D-5750	2. Government Accession No.	3. Recipient's Catalog No.

4. Title and Subtitle DRAG CHARACTERISTICS OF SEVERAL TOWED DECELERATOR MODELS AT MACH 3	5. Report Date May 1970
	6. Performing Organization Code

7. Author(s) Robert Miserentino and Herman L. Bohon	8. Performing Organization Report No. L-6664
9. Performing Organization Name and Address NASA Langley Research Center Hampton, Va. 23365	10. Work Unit No. 124-08-20-04-23
	11. Contract or Grant No.
12. Sponsoring Agency Name and Address National Aeronautics and Space Administration Washington, D.C. 20546	13. Type of Report and Period Covered Technical Note
	14. Sponsoring Agency Code

15. Supplementary Notes

Technical Film Supplement L-1075 available on request.

16. Abstract

An investigation has been made to determine the possibility of using toroid-membrane and wide-angle conical shapes as towed decelerators. Parameter variations were investigated which might render toroid-membrane models and wide-angle-cone models stable without loss of the high drag coefficients obtainable with sting-mounted models. The parameters varied included location of center of gravity, location of the pivot between the towline and the model, and configuration modifications of the aft end as the addition of a corner radius and the addition of a skirt. The toroid membrane can be made into a stable towed decelerator with a suitable configuration modification of the aft end. Cones with apex angles greater than 90° did not have improved values of drag coefficient even when somewhat stabilized by varying the corner radius or skirt.

17. Key Words (Suggested by Author(s)) Cones Tension shell Decelerator Supersonic deceleration	18. Distribution Statement Unclassified — Unlimited		
19. Security Classif. (of this report) Unclassified	20. Security Classif. (of this page) Unclassified	21. No. of Pages 33	22. Price* $3.00

DRAG CHARACTERISTICS OF SEVERAL TOWED

DECELERATOR MODELS AT MACH 3

By Robert Miserentino and Herman L. Bohon
Langley Research Center

SUMMARY

The toroid membrane (tension shell) and the wide-angle cone have been shown analytically and experimentally to have high free-body drag. An investigation has been made to determine the possibility of using these high-drag shapes as towed decelerators. Toroid-membrane models and some wide-angle-cone models towed behind a body at Mach 3 on a flexible towline exhibited highly unstable motion at all towline lengths. Parameter variations were investigated which might render toroid-membrane models and wide-angle-cone models stable without the loss of the high drag coefficients obtainable with sting-mounted models. The parameters varied included location of center of gravity, location of the pivot between the towline and the model, and configuration modifications of the aft end as the addition of a corner radius and the addition of a skirt.

It is concluded that the toroid membrane can be made into a stable towed decelerator with a suitable configuration modification of the aft end. The drag coefficients obtainable are from 1.3 to 1.5 which are less than those of the same models sting mounted, but above those of the towed 90° cone models. Cones with apex angles greater than 90° did not have improved values of drag coefficient even when somewhat stabilized by varying the corner radius or skirt. The motions of the towline and model system which determine performance are indicated.

INTRODUCTION

Future space-vehicle entry and descent systems may require aerodynamic decelerators to stabilize and decelerate entry capsules and instrument packages throughout a wide range of Mach numbers. The selection of the decelerator system will depend upon such basic factors as weight, drag, stability, and simplicity of design and construction.

Present towed supersonic decelerators consist of porous parachutes, such as the hemisflo, and of pressure vessels, such as the ballute (ref. 1). The drag performance of supersonic parachutes is limited by the requirement of high porosity and that of the ballute by the requirement of small apex angles to provide stability. Although the tension

shell shape has not been studied as a towed decelerator, it has been shown analytically to have high free-body drag capability at supersonic speed (ref. 2). This capability has been verified experimentally at Mach numbers 3 and 7 (refs. 3 and 4, respectively). The towed configuration (toroid membrane) would consist of a flexible-membrane shroud with a tension shell shape from reference 2 and a compression member, such as a pressurized toroid, at the rear edge.

An investigation to determine the stability and drag performance of toroid-membrane shapes as towed decelerators has been conducted at Mach 3. The models covered an array of membrane shapes designated by values of A^2 (the shape parameter from ref. 2) from 0.83 to 1.50 with zero circumferential stress. These shapes are shown in figure 1. Note that the lower the value of A^2, the blunter the decelerator. In an initial series of tests, the models with the configurations shown in figure 1 performed violent motions on a towline. The remainder of the toroid-membrane tests were performed with one shape to which modifications were made to render the decelerator stable. The shape $A^2 = 1.40$ was chosen since the sting-mounted counterpart showed a high drag coefficient (ref. 3). Only this portion of the toroid-membrane test program is reported herein.

Parameters investigated are center-of-gravity location of the model and location of the pivot between the towline and the model. Configuration modifications included variations in aft corner radius and the addition of a conical skirt. Also, blunt cones with apex angles from 80° to 120° were tested on a towline and a few unstable models were modified to permit comparison of the results with the toroid-membrane data.

The models were tested in the Langley 9- by 6-foot thermal structures tunnel at Mach 3 and dynamic pressures exceeding 1480 lbf/ft^2 (71.1 kN/m^2) and were attached to a strut-mounted forebody by a single flexible towline. The Reynolds number, based on the original model base diameter, was 3×10^6. The recorded data include the gross drag, drag variation, and motion pictures of model behavior. Motion-picture film supplement L-1075 has been prepared and is available on loan. A request card and a description of the film are included at the back of this paper.

<div align="center">SYMBOLS</div>

The units used for the physical quantities in this paper are given both in the U.S. Customary Units and in the International System of Units (SI). Factors relating the two systems are given in reference 5 and those used in the present investigation are presented in the appendix.

A^2	shape parameter associated with Newtonian pressure (see ref. 2)
C_D	drag coefficient, $\dfrac{D}{q\pi\left(r_b'\right)^2}$
D	drag
d	outside diameter of forebody
f_P	frequency of model pitching
f_R	frequency of model roving
k	radius of gyration of model mass about center of gravity
l	towline length
L_{cg}	distance from towline pivot to center of gravity
L_b	length of model base (see fig. 3(b))
L_3	distance between towline pivot and apex of original shape, measured in direction of airflow
m	total mass of model
q	free-stream dynamic pressure
q_o	free-stream dynamic pressure of 1482 lbf/ft^2 (70.96 kN/m^2)
r_b	base radius of original decelerator
r_b'	base radius of modified decelerator
r_c	corner radius at aft end of decelerator
Δ	deviation from average C_D
Φ	flare angle of decelerator skirt

θ cone angle of decelerator

γ roving angle

MODELS

The models tested were toroid-membrane models which conform to a tension shell shape factor $A^2 = 1.40$ for zero circumferential stress and cone models with apex angles from $80°$ to $120°$. (See table I of ref. 2 for coordinates of tension shell shapes.) Typical configurations are shown in figure 2 for the toroid-membrane models and the cone models. The cone models were made from mahogany and had a polished finish on the outer surface. The toroid-membrane models were formed on a mold from either glass fiber cloth or polyester cloth and impregnated with a stiff polyester resin. One flexible toroid-membrane model was fabricated with polyester cloth impregnated with rubber throughout the membrane shroud and with a stiff polyester resin throughout the toroid. All models were symmetric about their center line and had a nominal base radius r_b of 4.00 in. (10.16 cm).

Typical modifications to the original toroid-membrane shape are shown in figure 3(a). The original shape has a zero corner radius r_c at the base (surface ends at right angles to the center line). Modifications to the shapes shown in the first column involve increases in base corner radius so that these shapes represent toroidal rings. The shapes in the second and third columns show the addition of $5°$ and $15°$ flared skirts to the shapes of the first column. The shapes in the fourth column have reductions in base radius r_b' so that the surface at the base makes a reduced angle to the center line. For these reduced-base shapes the base corner radius r_c is zero.

Profile details at the base corner are illustrated in figure 3(b). All toroidal-ring shapes had a maximum base radius r_b' equal to the nominal base radius r_b. The $5°$ and $15°$ skirt shapes had a fixed position for the skirt in relation to the original shape which was independent of the corner radius. With no corner radius $(r_c = 0)$, the skirts intersect the original shape at $0.985r_b$.

Values of the model geometry variables are given in table I(a) for the toroid-membrane models and in table I(b) for the cone models. Also listed in table I for each model tested are the center-of-gravity location, pivot location, model mass, and the square of the radius of gyration about the center of gravity.

APPARATUS

A sketch of the test apparatus is shown in figure 4(a) and details of the strut and the forebody are given in figure 4(b). The models were towed behind the forebody with a

4

flexible 1/8-in-diameter (0.32 cm) steel aircraft cable. The model position behind the forebody was controlled by a motor-driven winch or air cylinder. Drag loads were measured with a strain-gage-type load cell and were recorded continuously on an oscillograph. The pulleys were ball-bearing mounted and induced very little error in the drag measurement. Model motion was recorded by motion-picture cameras operating at a speed of 400 frames per second.

The tests were conducted in the Langley 9- by 6-foot thermal structures tunnel which is a Mach 3 blowdown facility exhausting to the atmosphere. See reference 6 for a complete description of the facility. Generally, tests were made at the minimum free-stream dynamic pressure q_O of 1482 lbf/ft^2 (70.96 kN/m^2), a stagnation temperature of 300° F (420 K), and a Reynolds number, based on the original model base diameter, of approximately 3×10^6.

TEST PROCEDURE

During tunnel startup the model was securely held in a snugly fitting conical sleeve in the forebody (figs. 2 and 4) by pre-tension in the towline of 1000 lbf (4.4 kN). After the tunnel test conditions were established, the model was reeled out, with the winch, at a rate of approximately 4 in./sec (0.1 m/s) to a maximum distance of 40 in. (1.0 m) behind the forebody. Drag data were recorded continuously. The procedure was then reversed and the model was pulled securely into the forebody prior to shutdown. When the air cylinder was used, the models rapidly deployed to 20 in. (0.5 m) and data were recorded only at the rearmost position.

RESULTS AND DISCUSSION

Forty-five tests were conducted on toroid-membrane models and 22 tests on cone models; results of these tests are given in table II. Data tabulated are the ratio of towline length to forebody diameter l/d, the average of the drag coefficient C_D, the deviation from average drag coefficient Δ, and, where possible, frequency of model pitching f_P and frequency of model roving f_R.

Where l/d is given as a range, the values of C_D and Δ are representative over that range. The l/d range was either limited by the towline length or limited to cover the highest steady drag period. In general, if Δ was less than 0.04 throughout the tabulated l/d range, the drag behavior was classified as good stability. If Δ ranged from 0.04 to 0.10, it was classified as medium; if the range was above 0.10, it was classified as unstable. If Δ had two distinct values for more than 1/2 sec, then both classes of stability were listed although only the minimum value of Δ and the corresponding value of C_D were given.

The tabulated values of the frequencies were obtained for a specific l/d from the test motion-picture film and were measured only when motion was clearly discernible and uncoupled, except as noted in the table. As seen in table II the pitching frequency was high and varied between 24 and 119 Hz; the roving frequency range was between 6 and 33 Hz.

Model Behavior

Most models were reeled out to a desired location, held for a time, and then reeled in. During each test the model motion and drag loads were recorded continuously. When oscillatory motion occurred, it was characterized by either a pitching motion, a roving motion, or a combination of these motions. The pitching and roving motions are illustrated in figure 5. Pitching occurred as planar motion of the model about a point near the pivot and involved motion of the towline. Roving occurred as circular motion of the decelerator and towline about the axis of the forebody with the towline taut. It should be noted that the frequencies listed in table II do not necessarily imply an unstable condition since, in many tests, the motion was very quickly damped. Motion of the system did influence the drag results significantly and this is discussed in a subsequent section.

General model behavior is illustrated with the sample oscillograph record shown in figure 6 for toroid-membrane model 23. The smooth solid line indicates the model position behind the forebody l/d, and the line with oscillations is the drag recorded from the load cell output. The drag has been converted to C_D for convenience of discussion. The model was reeled out to $l/d = 10$ in about 7.5 sec, remained at that position for 5.5 sec, and then was reeled in. During reel out of the model, the drag load increases abruptly at $l/d = 5$ which defines the end of the forebody near-wake region. (See ref. 7 for a discussion of wake regions.) Also, this increase in drag is accompanied by an increase in the stability of the model (i.e., a decrease in the amplitude of the oscillations of the drag trace). In the region of $5 \leq l/d \leq 8$ the decelerator was pitching and the drag level was not high. In this region the average C_D is 0.9 and Δ is ± 0.08. At $l/d \approx 8$ the pitching motion ceased and the drag increased to the maximum value. The random spikes in the drag trace for l/d between 8 and 10 occur when the decelerator goes through several cycles of highly damping pitching motion. When pitching begins, the drag level suddenly decreases to that value at l/d between 5 and 8. When pitching ceases the drag level again increases. Similar model behavior at different towline lengths has been demonstrated analytically in reference 8. Model behavior like that represented by the trace for l/d between 5 and 8 would be classified as unstable in table II. The behavior for l/d between 8 and 10 would be classified as good or medium stability.

6

Several significant observations were made from correlating motion pictures with oscillograph traces such as figure 6. First, a model may be stable at one value of l/d and be unstable at a different towline length. Second, the pitching motion of a towed decelerator is detrimental to the drag coefficient. Third, the high drag values occur when the model is either steady and directly behind the forebody or when the model is roving. Finally, when the roving half-angle (fig. 5) increased beyond approximately 4°, a pitching motion would occur and suddenly reduce the drag load and roving motion.

Stability and Drag of Toroid-Membrane Models

Although the original tension shell shape appeared attractive as a towed decelerator because it had a high C_D when sting mounted, it was highly unstable on a towline. Modifications which were made to achieve stability included increasing the base corner radius r_c, adding skirts to the base, and reducing the base radius (fig. 3). Also, small changes were made in the center-of-gravity location and the location of the pivot between the towline and the rigid model. Effects of these modifications on the stability and drag of toroid-membrane decelerators are presented and discussed in this section.

Effects of base corner radius and skirt.- The oscillograph trace in figure 7(a) shows the recorded drag history of toroid-membrane model 1 which had a corner radius r_c of $0.06r_b$ and no skirt (second model in col. 1 of fig. 3(a)). As can be seen the model motion was highly oscillatory and erratic at all towline lengths. The average C_D was 1.20 for constant towline length and the deviation Δ was 0.43. The drag history shown in figure 7(b) is for model 10 which had the same corner radius r_c of $0.06r_b$ as model 1 but was modified by the addition of a 5° flare skirt 1 in. (2.5 cm) long. Note that stability was improved and is listed as medium in table II. If the spikes were ignored, the average C_D was 1.28 and Δ was 0.05. When the corner radius r_c was increased to $0.19r_b$ (model 17), the stability was good for l/d between 9 and 12 as shown in figure 7(c). The average C_D was 1.26 and Δ was 0.02.

The results presented in figure 8 show the effects of corner radius r_c and skirt flare angle Φ on drag and stability. The average C_D and deviation Δ are plotted against r_c/r_b for three model configurations at $l/d = 10$. The initial increases in corner radius caused a decrease in the magnitude of the pitching motion as indicated by the decrease in the drag deviation. At $r_c/r_b = 0.19$, all models were stable and further increases in corner radius resulted in a decrease in C_D as would be expected. For toroidal-ring models, the maximum drag coefficient of 1.31 was obtained for $r_c/r_b = 0.16$ and the model had medium stability. The solid circles are data from reference 7 for sting-mounted toroidal-ring models and indicate considerably higher C_D values than those of the towed models.

Effect of base radius reduction.- Another series of models was modified by reducing the base diameter by simply cutting off the original shape (fourth col. of fig. 3(a)). Since theoretically a tension shell membrane must intersect the base ring with a tangent perpendicular to the axis of revolution (ref. 2), these cut-off shapes may be more difficult to achieve in practice and may require a more complex structure. The results of base radius reduction (for models 26 to 44) are shown in figure 9 wherein C_D and Δ are plotted against r'_b/r_b at $l/d = 8$.

The dash-line curve (from ref. 7) represents values of C_D that were obtained when similar shaped models were sting mounted. For $\dfrac{r'_b}{r_b} > 0.88$, the models were extremely unstable as indicated by the large values of Δ. Models with r'_b/r_b below 0.87 had medium stability and values of C_D from 1.40 to 1.55. The solid line is faired through some of the data from models with the highest drag coefficient. The highest drag coefficient for a stable model $\left(C_D = 1.55\right)$ was obtained for a toroid-membrane model cut off at 87 percent of the original base radius. For r'_b/r_b from 0.83 to 0.87, the measured C_D values of the towed models agree reasonably well with the measured C_D values of the sting-mounted models from reference 7.

Effects of pivot point and center of gravity.- A modified toroid membrane having medium stability (models 10 to 14) was tested for various values of L_3, the distance between the apex of the rigid model and the towline pivot. The resulting variations of C_D and Δ with L_3/r_b are shown in figure 10. A slight increase in C_D and stability is shown when the pivot is located ahead of the model apex. However, increases in L_3/r_b beyond 0.1 resulted in large reductions in C_D and a degradation of stability. It is concluded from figure 10 that only a limited increase in stability can be obtained by extending the stiff front of this towed decelerator configuration.

The effect of variation of the center-of-gravity location on C_D and Δ is shown in figure 11 for toroid-membrane models with a toroidal ring (models 5 to 8). The models with $r_c/r_b = 0.19$ and a pivot location at the model apex $\left(L_3/r_b = 0\right)$ were tested at $l/d = 10$. The figure shows that the variation of L_{cg} from $0.84r_b$ to $1.7r_b$ had a negligible effect on C_D and Δ.

Effect of model flexibility.- The usefulness of a toroid-membrane decelerator depends on the membrane and toroid being flexible and foldable (ref. 9). One model tested (model 45) was made from polyester cloth with a rubber-impregnated membrane between the nose and a rigid base skirt. A photograph of the model is shown as figure 12. The model had a small corner radius $\left(r_c = 0.06r_b\right)$, the pivot at the apex $\left(L_3/r_b = 0\right)$, and a cylindrical skirt ($\Phi = 0$). The model performance was very similar to that obtained for the rigid model with the same corner radius and a 5° flared skirt (model 10). The C_D obtained was 1.25 with good to medium stability. No relative motions between the stiff

skirt and flexible membrane was discernible. Thus, such flexibility does not appear to be detrimental.

Stability and Drag of Cone Models

A series of cone models was tested to provide data comparable with data for the toroid-membrane models. Cone apex angles ranged from 80° to 120°. The measured values of C_D and Δ are shown in figure 13 for the test range of cone angles (circle symbols). The dash-line curve and the diamond symbols, respectively, indicate experimental data obtained with sting-mounted models at a low Reynolds number (ref. 10) and at a Reynolds number similar to that of the present tests (refs. 3 and 11). The triangle symbol represents data obtained with a towed 80° cone at a Reynolds number similar to that of the present tests; this model was towed behind a more streamlined forebody (ref. 12) than that used in these tests.

The present drag data are in good agreement with data from previous tests with both towed and sting-mounted models for values of θ up to 90° and indicate little or no effect of the forebody wake and towline. However, as the cone angle θ increased above 90°, the towed cone models became unstable in pitch (which increased in severity as θ increased) with a resultant sizable reduction in the average C_D and a corresponding increase in Δ. The differences in values of C_D of the towed models and those of the sting-mounted models increased for $\theta > 90^O$. Motion pictures showed that for all unstable motion of the model, the towline also experienced large amplitude sinusoidal motion. The 90° cone had good stability and a drag coefficient of 1.09.

Attempts were made to produce stability by varying L_3 on the 95° cone and by adding 5° and 15° flared skirts with varying corner radius on the 100° cone (tables I(b) and II(b), models 11 to 22). None of these modifications controlled the pitching.

CONCLUDING REMARKS

An experimental investigation has been carried out at Mach 3 to determine the stability and drag performance of towed decelerators having toroid-membrane and conical shapes. The toroid-membrane models conformed to a tension shell shape modified in various ways at the base to simulate a large pressurized toroid or other compression member. The cone models had apex angles from 80° to 120°. All models were fabricated as rigid bodies except one which was fabricated to simulate membrane flexibility. The models were towed behind a slender forebody with a flexible towline of varying length. Drag data were recorded continuously on an oscillograph and model motion was recorded by high-speed movie cameras.

The models having the basic tension shell shape were unstable and exhibited large-amplitude pitching motion. All modifications which resulted in stable behavior were such as to reduce the drag coefficient of the basic shape from the value obtained from free-body or sting-mounted models. However, a high drag coefficient of 1.3 was obtained for a stable model having a corner radius 15 percent of the model base radius. Toroid-membrane models modified by flared skirts also exhibited stable behavior although the maximum drag coefficient was somewhat less.

The highest drag coefficient for a stable model $(C_D = 1.55)$ was obtained for a toroid-membrane model cut off at 87 percent of the original base diameter. However, this shape modification may be impractical to achieve with a flexible membrane and a deployable, inflatable toroid.

Towed cones with apex angle greater than 90° were unstable and geometric modifications similar to those which stabilized the toroid membrane did not stabilize the cone. The drag coefficient of the stable 90° towed cone was about 1.1.

Model instability caused by pitching or roving motions was found to be dependent on position behind the payload. Models stable at one ratio of towline length to forebody diameter l/d may be unstable at a different l/d. The drag level varies with l/d beyond the near wake for the different modified models. Pitching motion was detrimental and caused a large reduction in drag. Small roving motion did not produce a loss in drag; however, if the roving half-angle exceeded approximately 4°, a pitching motion occurred which suddenly reduced the drag and roving motion. Therefore, the dynamics of a towed decelerator system are very significant and knowledge of the parameters influencing the motions is mandatory.

Langley Research Center,
    National Aeronautics and Space Administration,
        Hampton, Va., April 1, 1970.

APPENDIX

CONVERSION OF U.S. CUSTOMARY UNITS TO SI UNITS

The International System of Units (SI) was adopted by the Eleventh General Conference on Weights and Measures, Paris, October 1960 (ref. 5). Conversion factors for the units used herein are given in the following table:

Physical quantity	U.S. Customary Unit	Conversion factor (*)	SI Unit
Frequency	cps	1	hertz (Hz)
Length, radius	in.	0.0254	meters (m)
Pressure	lbf/ft^2	47.880258	newtons/meter^2 (N/m^2)
Temperature	$^{\circ}F$	$\frac{5}{9}(F + 459.67)$	Kelvin (K)
Force (load, drag)	lbf	4.44822	newtons (N)
Mass	lbm	0.453592	kilograms (kg)

*Multiply value given in U.S. Customary Unit by conversion factor to obtain equivalent value in SI Unit.

Prefixes to indicate multiples of units are as follows:

Prefix	Multiple
kilo (k)	10^3
centi (c)	10^{-2}

REFERENCES

1. Amer. Power Jet Co.: Performance of and Design Criteria for Deployable Aerodynamic Decelerators. ASD-TR-61-579, U.S. Air Force, Dec. 1963. (Available from DDC as AD 429 921.)

2. Anderson, Melvin S.; Robinson, James C.; Bush, Harold G.; and Fralich, Robert W.: A Tension Shell Structure for Application to Entry Vehicles. NASA TN D-2675, 1965.

3. Deveikis, William D.; and Sawyer, James Wayne: Aerodynamic Characteristics of Tension Shell Shapes at Mach 3.0. NASA TN D-3633, 1966.

4. Robinson, James C.; and Jordan, Alfred W.: Exploratory Experimental Aerodynamic Investigation of Tension Shell Shapes at Mach 7. NASA TN D-2994, 1965.

5. Comm. on Metric Pract.: ASTM Metric Practice Guide. NBS Handbook 102, U.S. Dep. Com., Mar. 10, 1967.

6. Schaefer, William T., Jr.: Characteristics of Major Active Wind Tunnels at the Langley Research Center. NASA TM X-1130, 1965.

7. Sawyer, James Wayne; and Deveikis, William D.: Effects of Configuration Modifications on Aerodynamic Characteristics of Tension Shell Shapes at Mach 3.0. NASA TN D-4080, 1967.

8. MacNeal, Richard H.: The Flutter of Towed Rigid Decelerators. NASA CR-766, 1967.

9. Kyser, Albert C.: Deployment Mechanics for an Inflatable Tension-Cone Decelerator. NASA CR-929, 1967.

10. Owens, Robert V.: Aerodynamic Characteristics of Spherically Blunted Cones at Mach Numbers From 0.5 to 5.0. NASA TN D-3088, 1965.

11. Deveikis, William D.; and Sawyer, James Wayne: Effects of Cone Angle, Base Flare Angle, and Corner Radius on Mach 3.0 Aerodynamic Characteristics of Large-Angle Cones. NASA TN D-5048, 1969.

12. Charczenko, Nickolai: Aerodynamic Characteristics of Towed Spheres, Conical Rings, and Cones Used as Decelerators at Mach Numbers From 1.57 to 4.65. NASA TN D-1789, 1963.

TABLE I.- GEOMETRICAL CHARACTERISTICS

(a) Toroid-membrane models

Model	Φ, deg	r_c/r_b	r'_b/r_b	L_b/r_b	L_3/r_b	L_{cg}/r_b	m grams	lbm	k^2
1	†N.A.	0.06	1.00	0.06	0	0.907	1181	2.60	0.1255
2	↓	.09	↓	.09	0	.906	1194	2.63	.1563
3	↓	.13	↓	.11	.062	.815	734	1.62	.3244
4	↓	.16	↓	.13	0	.888	880	1.94	.2420
5	↓	.19	↓	.16	0	.837	751	1.66	.1929
6	↓	.19	↓	.16	0	1.250	901	1.99	.4814
7	↓	.19	↓	.16	0	1.500	899	1.98	.4978
8	↓	.19	↓	.16	0	1.688	900	1.98	.8629
9	↓	.22	↓	.19	0	.873	894	1.97	.2884
10	5	0.06	1.02	0.25	0	0.736	804	1.77	0.2274
11	↓	.06	↓	.25	-.094	.601	809	1.78	.2354
12	↓	.06	↓	.25	.094	.801	809	1.78	.2452
13	↓	.06	↓	.25	.188	.920	864	1.91	.2532
14	↓	.06	↓	.25	.250	.966	922	1.81	.2194
15	↓	.06	↓	.25	0	1.250	897	1.98	.4713
16	↓	.13	↓	.28	0	.625	650	1.43	.4400
17	↓	.19	↓	.31	0	.904	899	1.98	.1573
18	↓	.25	↓	.30	.094	.886	903	1.99	.1715
19	↓	.28	↓	.30	0	.859	900	1.98	.1779
20	15	0.06	1.07	0.31	0	0.634	906	2.00	0.1837
21	↓	.06	↓	.25	↓	.850	992	2.19	.2393
22	↓	.06	↓	.25	↓	1.118	992	2.19	.4551
23	↓	.13	↓	.25	↓	.802	376	.83	.3529
24	↓	.19	↓	.31	↓	.875	895	1.97	.1610
25	↓	.25	↓	.31	↓	.884	877	1.93	.1608
26	0	0	1.00	0.01	0	0.650	684	1.51	0.1208
27	↓	↓	.98	.07	↓	.632	696	1.53	.1439
28	↓	↓	.97	.01	↓	.619	499	1.10	.2062
29	↓	↓	.96	.08	↓	.617	682	1.50	.1584
30	↓	↓	.95	.01	↓	.633	612	1.35	.1860
31	↓	↓	.92	.01	↓	.617	627	1.38	.0771
32	↓	↓	.88	.01	↓	.505	641	1.41	.1258
33	↓	↓	.87	.01	↓	.627	375	.83	.1643
34	↓	↓	.87	.01	↓	.569	614	1.35	.1361
35	↓	↓	.87	.01	↓	.542	382	.84	.1802
36	↓	↓	.86	.01	↓	.573	610	1.35	.1016
37	↓	↓	.86	.01	↓	.576	388	.86	.1788
38	↓	↓	.85	.01	↓	.555	495	1.09	.0965
39	↓	↓	.85	.01	↓	.555	495	1.09	.0965
40	↓	↓	.85	.01	↓	.557	373	.82	.1789
41	↓	↓	.83	.01	↓	.567	355	.78	.1889
42	↓	↓	.83	.01	↓	.553	432	.95	.1373
43	↓	↓	.83	.01	↓	.527	457	1.01	.1369
44	↓	↓	.83	.01	↓	.414	512	1.13	.1124
45	*0	0.06	1.00	0.450	0	1.001	865	1.91	0.3219

†Not applicable.

*Flexible model.

TABLE I.- GEOMETRICAL CHARACTERISTICS – Concluded

(b) Cone models

Model	θ, deg	Φ, deg	r_c/r_b	r'_b/r_b	L_b/r_b	L_3/r_b	L_{cg}/r_b	m grams	m lbm	k^2
1	80	0	0	1.00	0.03	0	0.910	1080	2.38	0.2515
2	85	↓	↓	.99	.06	.375	1.200	1008	2.22	.2644
3	90			1.00	.03	0	.816	960	2.11	.2418
4	92			1.00	.03	0	.773	851	1.88	.2163
5	95			.99	.06	0	.769	886	1.95	.2107
6	100			1.00	.03	0	.666	762	1.68	.1860
7	105			1.00	.03	.063	.709	843	1.86	.2107
8	110			1.00	.03	0	.613	755	1.66	.2007
9	115			1.00	.03	0	.501	630	1.39	.2019
10	120	↓	↓	1.00	.03	0	.481	614	1.35	.1894
11	95	0	0	0.99	0.06	0.125	0.869	886	1.95	0.2184
12	↓	↓	↓	↓	↓	.250	.982	886	1.95	.2133
13						.375	1.121	886	1.95	.1867
14	↓	↓	↓	↓	↓	.500	1.185	886	1.95	.2349
15	100	5	0.06	1.03	0.25	0	0.823	1208	2.66	0.2515
16	↓	5	.13	1.03	↓	↓	.823	1211	2.67	.2544
17		5	.19	1.03			.821	1206	2.66	.2528
18		5	.25	1.07			.792	1194	2.63	.2623
19		5	.31	1.07			.796	1195	2.63	.2439
20		15	.06	1.07			.822	1210	2.67	.2519
21	↓	15	.13	1.07			.823	1212	2.67	.2570
22	↓	15	.19	1.07	↓	↓	.828	1234	2.72	.2571

TABLE II.- TEST DATA

(a) Toroid-membrane models

$$\left[q_o = 1482 \text{ lbf/ft}^2 \quad (70.96 \text{ kN/m}^2)\right]$$

Model	l/d	Average C_D	Δ	Good stability	Medium stability	Unstable	f_P, Hz	l/d	f_R, Hz	γ, deg	l/d
1	5 to 10	1.20	0.43			X	*		*		
2	5 to 10	1.24	.21			X	*	10	*		10
							82	10	8	12	10
3	8 to 16	1.28	.04	X	X		74	16	14	5.7	16
4	5 to 12	1.31	.06		X	X	*	12	*		12
							67	12	17	1.8	12
5	5 to 12	1.28	.03	X			*	12	17	3.5	12
6	5 to 12	1.27	.04	X	X				29	Varied	12
7	5 to 12	1.26	.035	X	X		Random		Random		
8	5 to 12	1.27	.03	X	X		Small amplitude				
9	5 to 12	1.22	.03	X			Random		Random		
10	8 to 10	1.28	0.05		X	X	114	5	23	5	7
11	10 to 16	1.23	.08		X	X	*		*		
12	10 to 15	1.32	.04	X	X		66	10	*		15
							82	14			
13	6 to 8	1.21	.06		X		*	8	15.1	5.6	7
14	4 to 12	1.06	.04	X			80	12	15		10
15	10 to 12	1.21	.08		X		*	12	13	13	12
							66	12			
16	6 to 14	1.21	.04	X			66	14			
17	5 to 12	1.26	.02	X					17	1.7	12
18	5 to 12	1.24	.03	X	X		*		*		
19	5 to 12	1.19	.02	X			None		14	2.3	12
20	10 to 12	0.90	0.30		X	X	85	12		None	
21	10 to 12	1.21	.01	X	X		77	12		None	
22	10 to 12	1.20	.01	X	X		80	16			
23	8 to 10	1.14	.02	X			100	10			
24	5 to 12	1.12	.03	X	X		Random		Random		
25	5 to 12	1.08	.02	X	X		Small amplitude	5 to 12			
26	†8	1.23	0.43			X	64	8	17		8
27		1.18	.47			X	94	8	16		8
28		1.22	.42			X	119	8	17		8
29		1.21	.50			X	108	8	18		8
30		1.14	.55			X	72	8	12		8
31		1.15	.57			X	80	8	20		8
32		1.55	.35			X	92	8	10		8
33		1.46	.14			X	61	8	14		8
34		1.55	.05		X		92	8	14		8
35		1.43	.33			X	78	8	13		8
							43				
36		1.44	.10		X		48	8	12		8
37		1.50	.10		X		61	8	15		8
38		1.52	.09		X		45	8	6		8
									15		8
39		1.42	.04	X			24	8	14		8
40		1.51	.03	X			44	8	17		8
41		1.46	.08		X		50	8	17		8
42		1.47	.04	X			34	8	16		8
							48				
43		1.49	.07		X		45	8	15		8
44		1.45	.06		X		35	8	15		8
45	5 to 10	1.25	0.01	X	X						

*Pitching and roving motion coupled.

†Deployment by air cylinder.

TABLE II.- TEST DATA — Concluded

(b) Cone models

$$\left[q_0 = 1482 \text{ lbf/ft}^2 \quad (70.96 \text{ kN/m}^2)\right]$$

Model	θ, deg	l/d	Average C_D	Δ	Good stability	Medium stability	Unstable	q/q_0	f_P, Hz	l/d	f_R, Hz	γ, deg	l/d
					Drag behavior				Pitching		Roving		
1	80	5 to 16	0.965	0.008	X			1.0	69	16			
2	85	†14	1.03	.01	X			1.0					
3	90	†8	1.09	.02	X			1.0					
4	92	5 to 10	1.00	.08		X	X	1.0	47	10			
5	95	5 to 8	.99	.09		X	X	1.7	114	10			
6	100	5 to 12	.97	.13			X	1.0	60	10			
7	105	5 to 18	.97	.10			X	1.0 1.5	80 100	16 16			
8	110	4 to 12	1.00	.18			X	1.0	45	12			
9	115	4 to 10	.97	.17			X	1.0	56	10			
10	120	4 to 10	1.00	.22			X	1.0					
11	95	4 to 10	0.99	0.07		X	X	1.66	74	10			
12	↓	↓	1.03	.05		X	X	1.0	92	10			
13			1.00	.06		X	X	1.0 1.66	98	10			
14	↓	↓	.95	.04		X	X	1.5 2.0	110	10			
15	100	4 to 10	0.94	0.08		X	X	2.0	95	10			
16	↓	↓	1.03	.07		X	X	2.25	114	10	33	2.8	10
17			.94	.11			X	1.62	87	10			
18			.89	.06		X	X	1.0	53	10			
19			.84	.05		X	X	1.0	66	10			
20			.87	.10			X	1.08	88	10			
21			.90	.10			X	2.0	100	10			
22	↓	↓	.89	.09		X	X	1.26	80	10			

†Deployment by air cylinder.
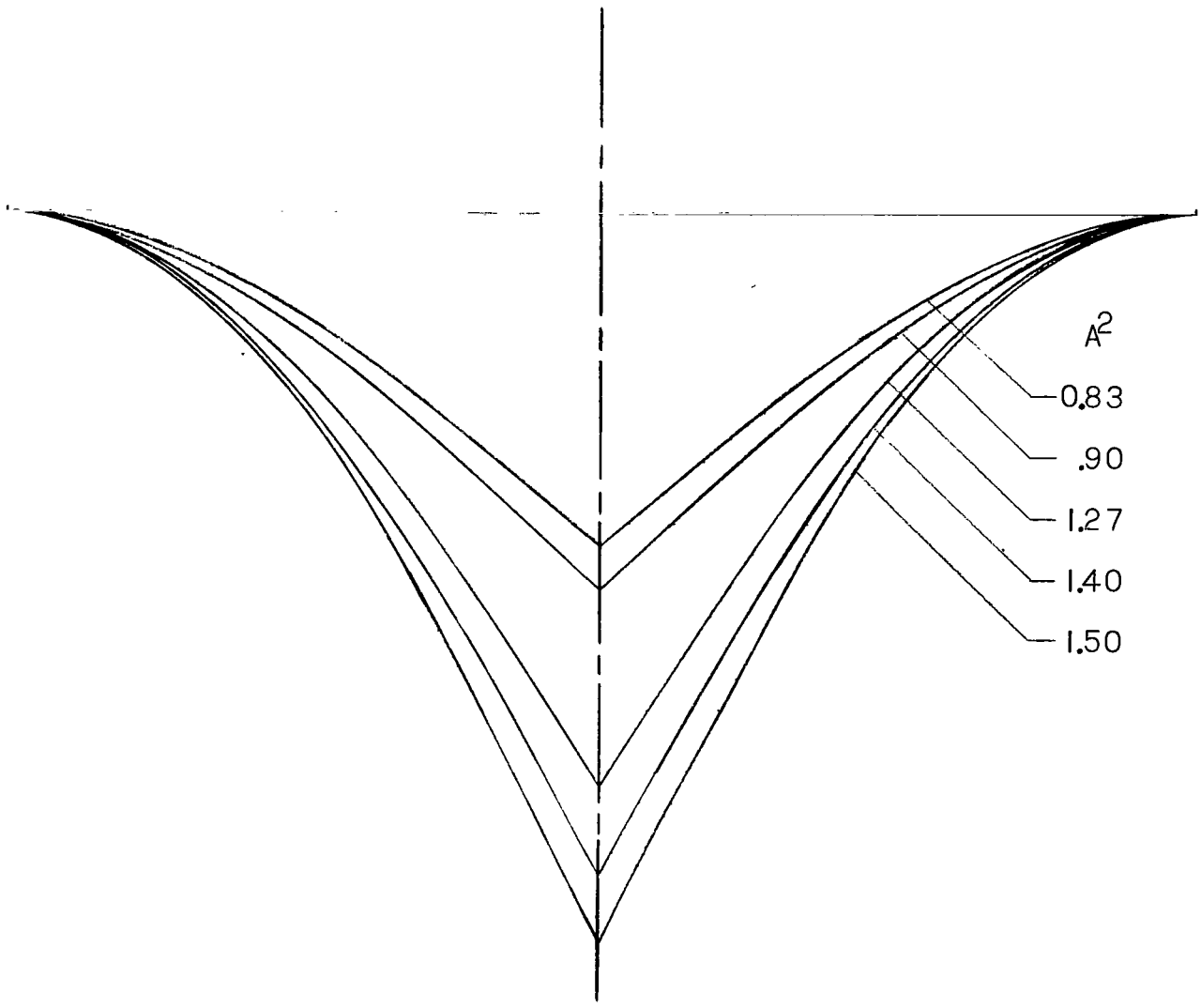
Figure 1.- Variations of membrane shape (zero circumferential stress).

$r_b = 4.00$ in. (10.16 cm)

r_b'

Φ

r_c

L_b

4.64 in. (11.79 cm)

L_{cg}

L_3

$55° 24'$

Airflow

d

l

FOREBODY

CONICAL SLEEVE
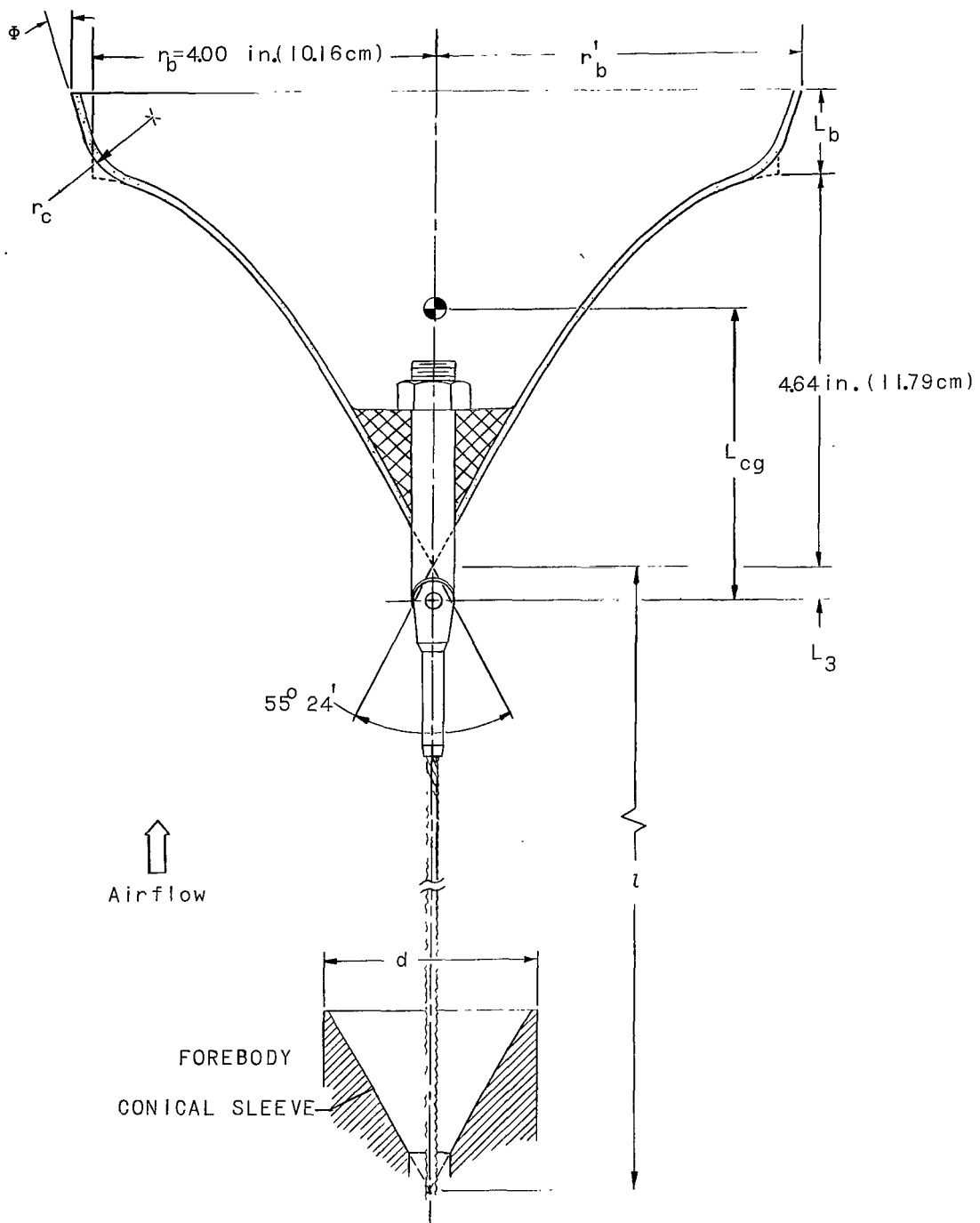
(a) Toroid-membrane model.

Figure 2.- Typical configurations with towline.
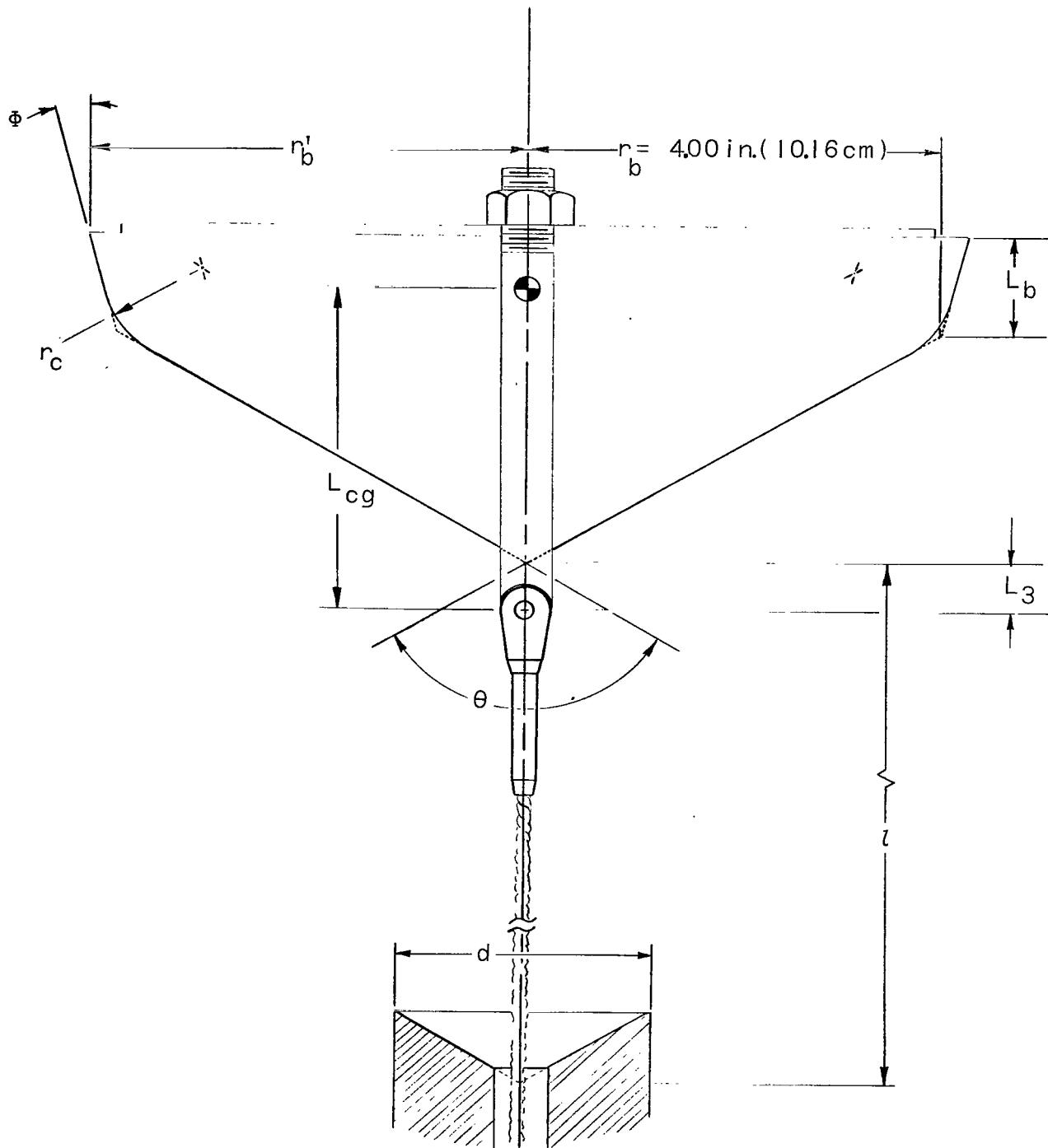
(b) Cone model.

Figure 2.- Concluded.

Toroidal ring   5° skirt   15° skirt   Reduced base

(Original shape)   (Original shape)

$\dfrac{r_c}{r_b} = 0$ $\dfrac{r_c}{r_b} = 0$ $\dfrac{r_c}{r_b} = 0$ $\dfrac{r_b'}{r_b} = 1.0$

.06   .06   .06   .95

.13   .12   .12   .90

.28   .25   .25   .85
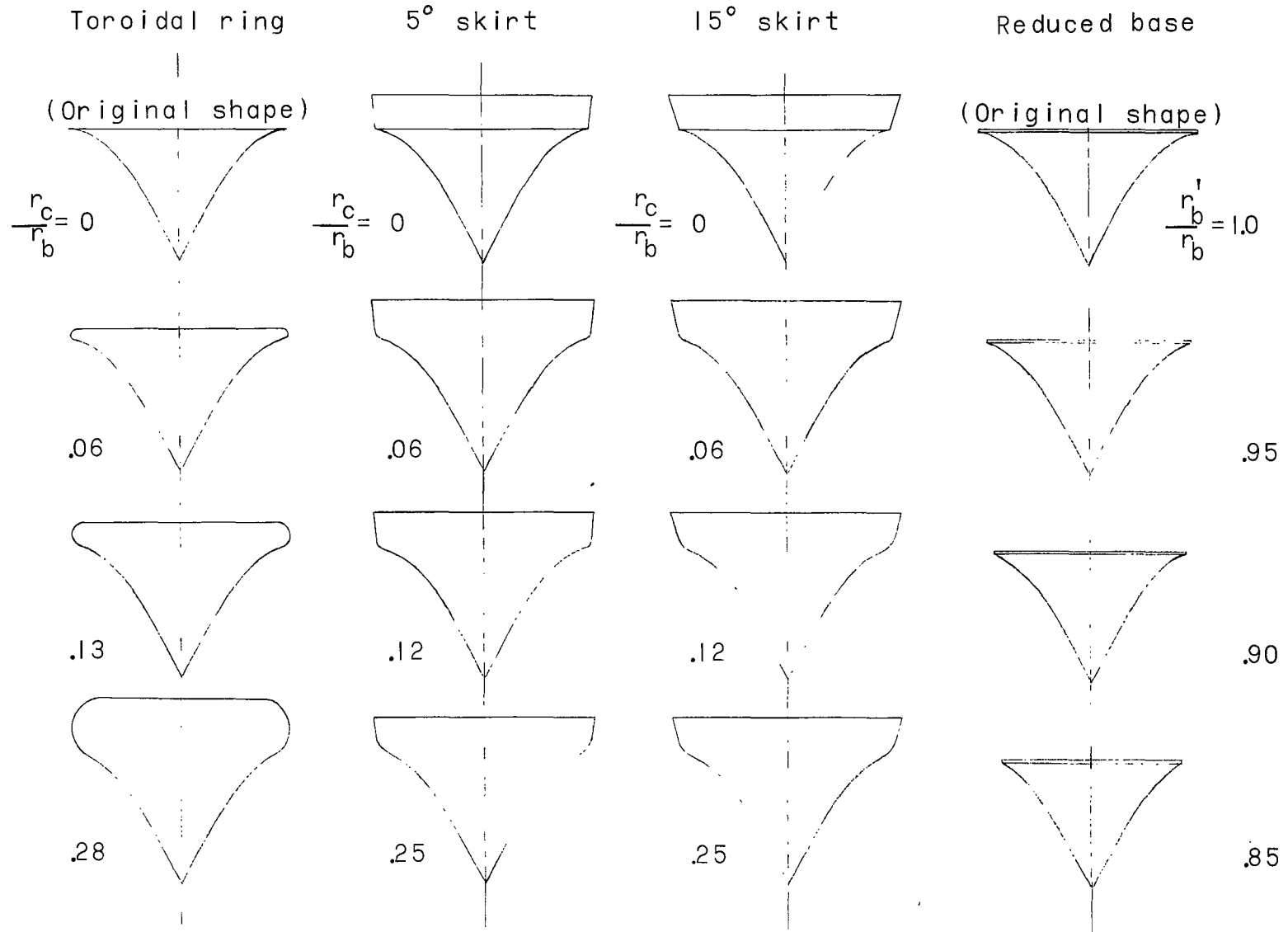
(a) Typical array of modifications to original shape.

Figure 3.- Toroid-membrane configurations.

Toroidal ring   5° skirt

15° skirt   Reduced base
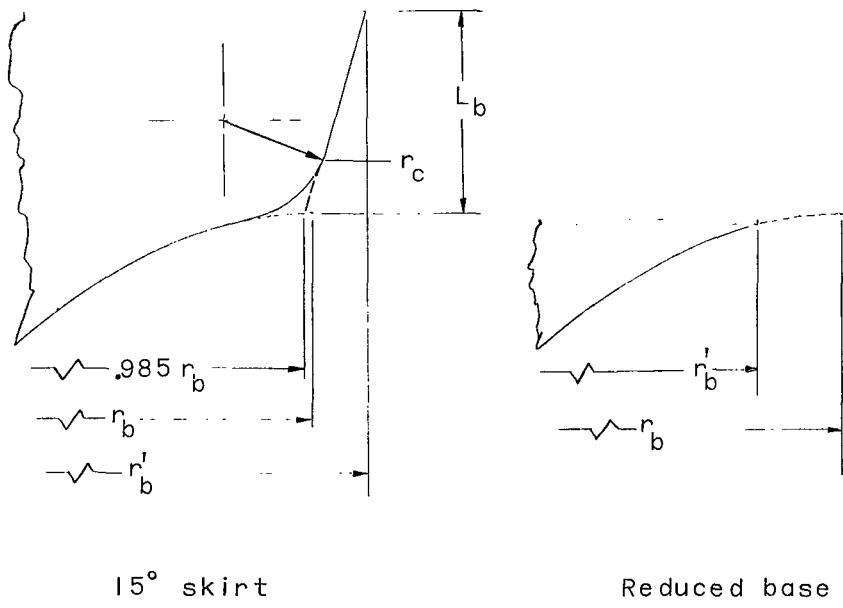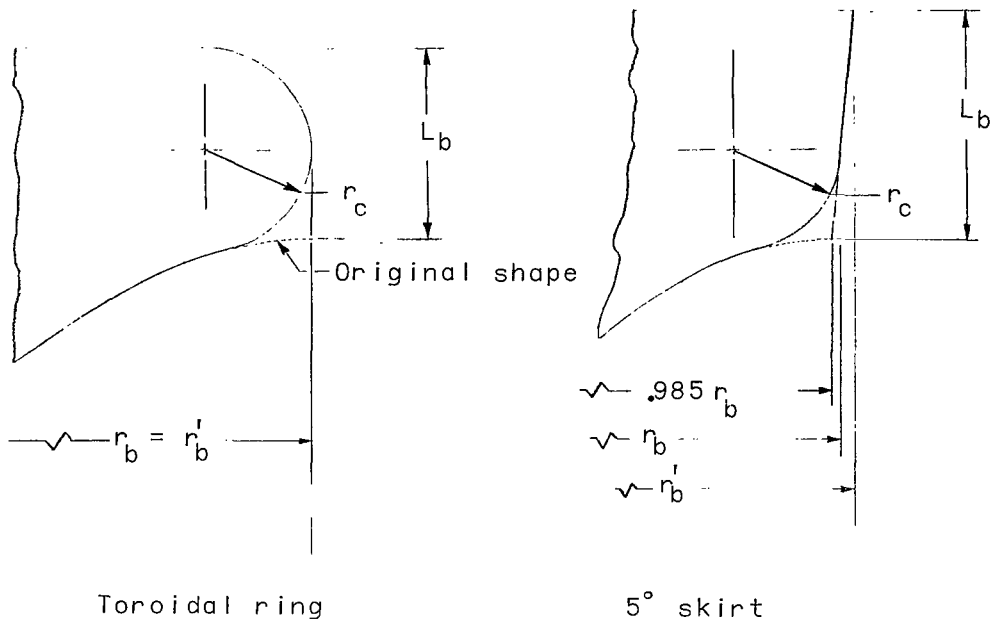
(b) Profile details of model corners.

Figure 3.- Concluded.

21
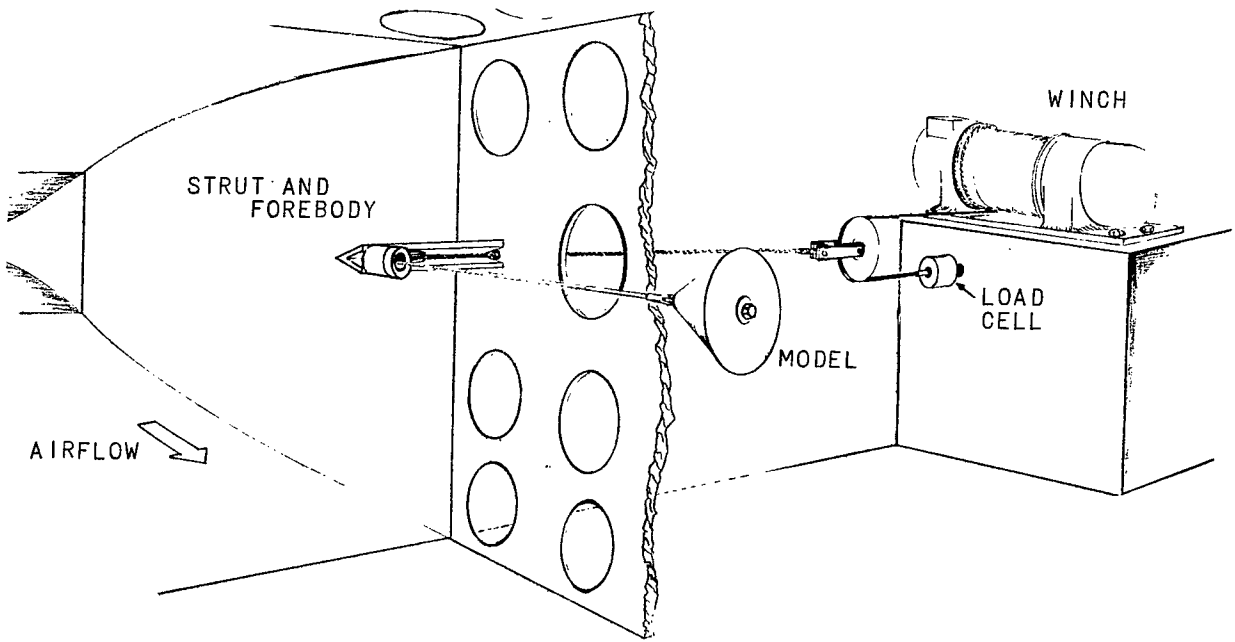
(a) Sketch of test apparatus.

2,37 (6,0)

STRUT

FOREBODY

TUNNEL
WALL

d=2,50
(6,35)

4,00 (10,16)

11,50 (29,21)

5,00 (12,7)

18,81 (47,8)

20,0 (50,8)
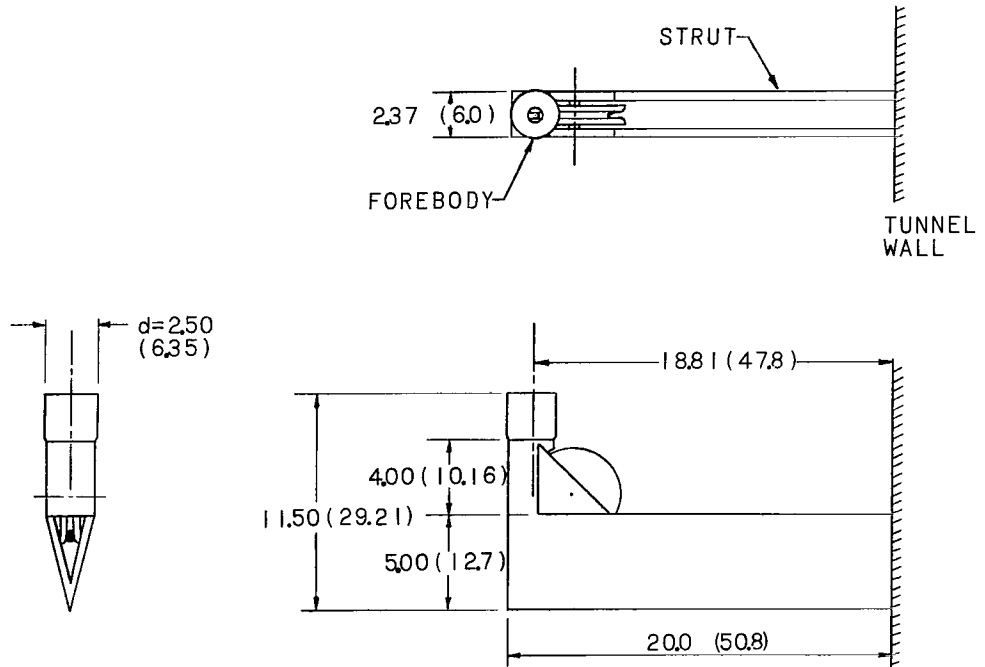
(b) Three-view drawing of strut and forebody.

Figure 4.- Test apparatus. Dimensions are given in inches and parenthetically in centimeters.
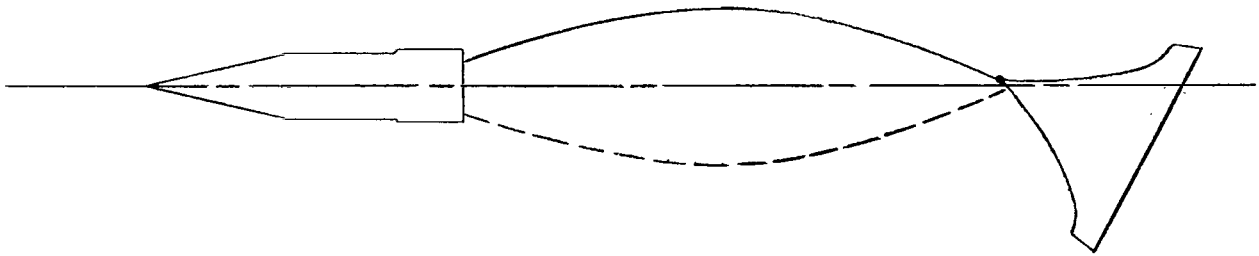
Pitch motion
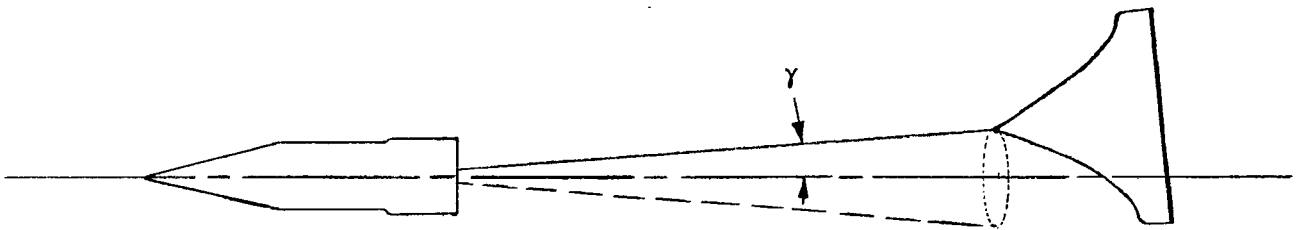
Roving motion

Figure 5.- Typical towed decelerator motions.
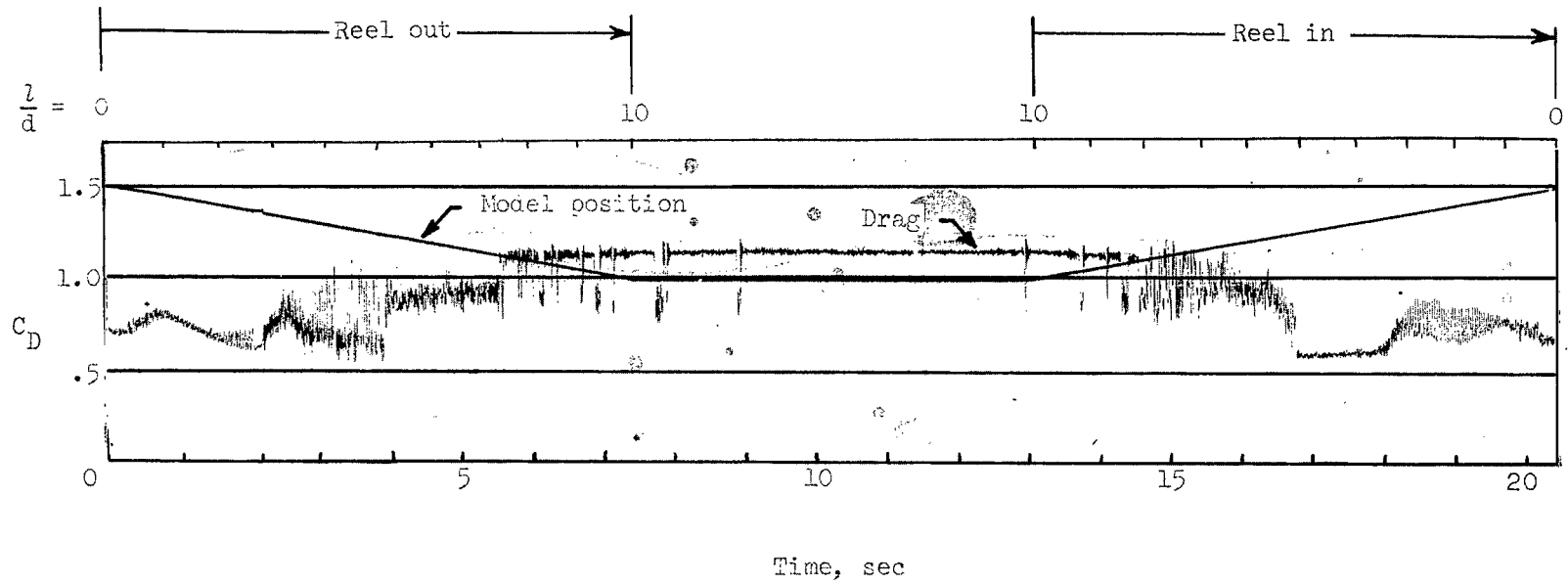
Figure 6.- Sample oscillograph record of general model behavior. Model 23.
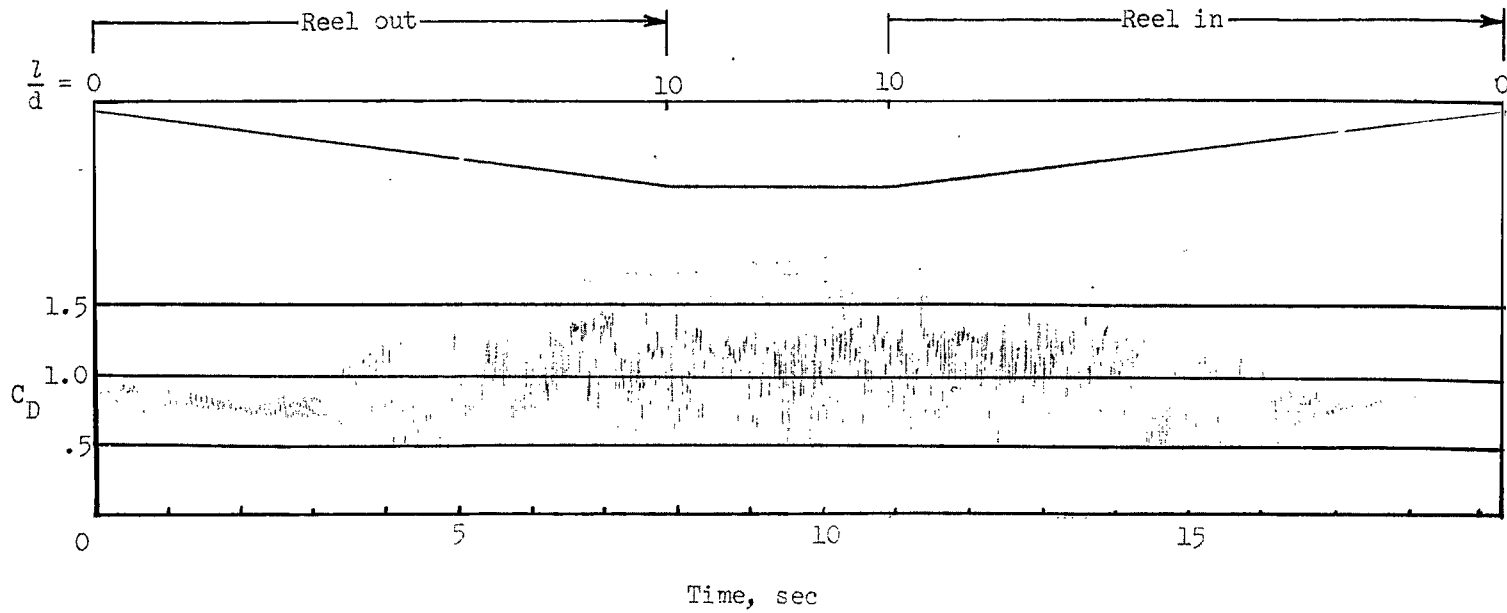
(a) Model 1.

Figure 7.- Sample oscillograph records showing effect of base corner radius and skirt.
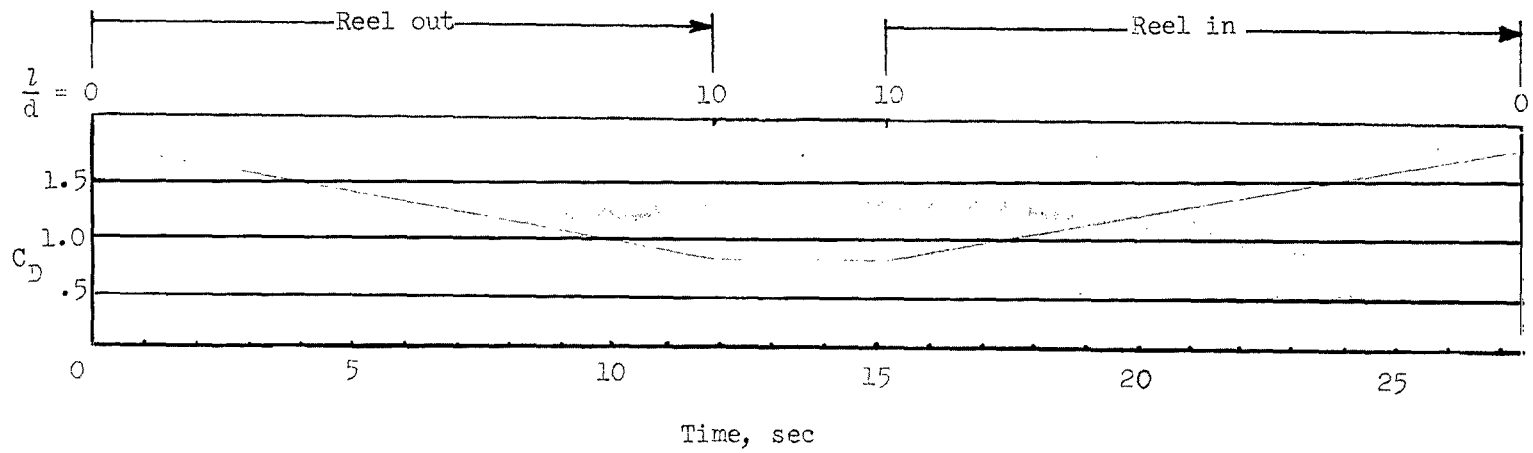
(b) Model 10.

Figure 7.- Continued.
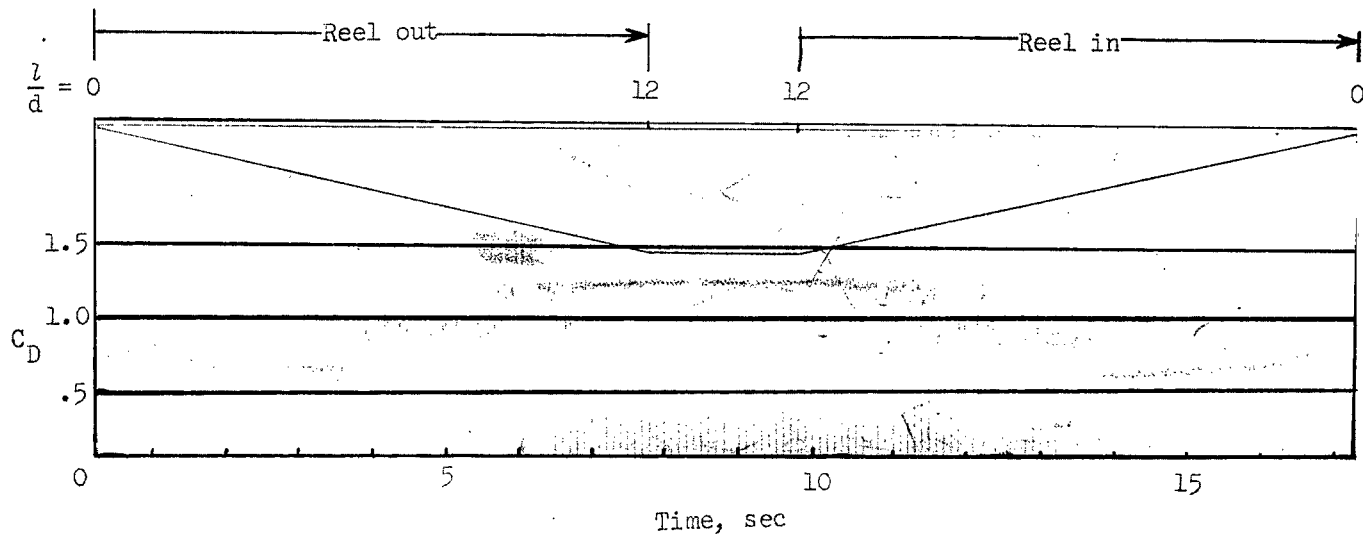
(c) Model 17.

Figure 7.- Concluded.
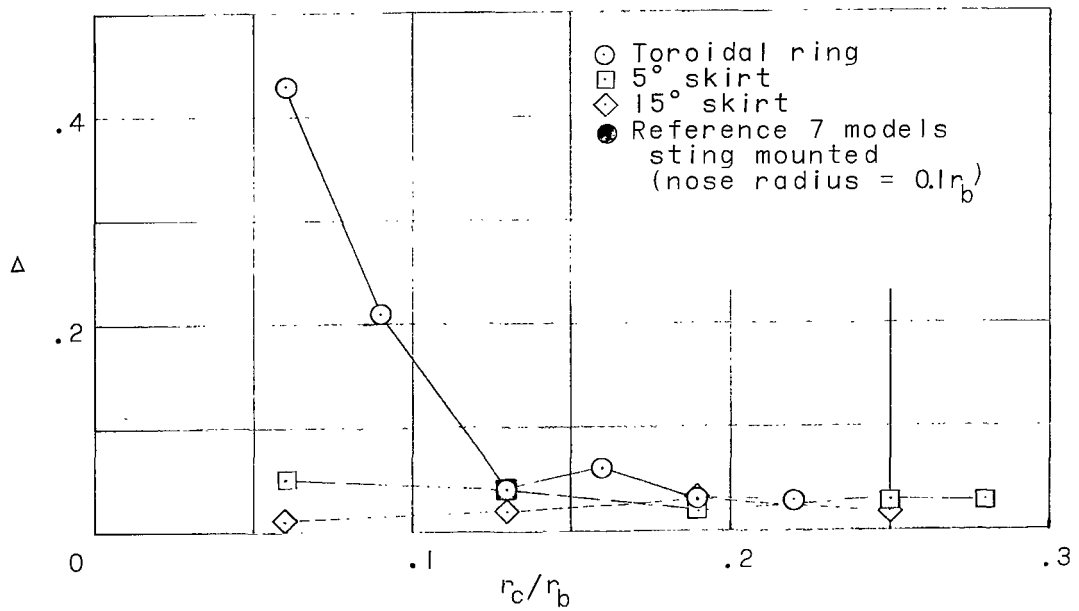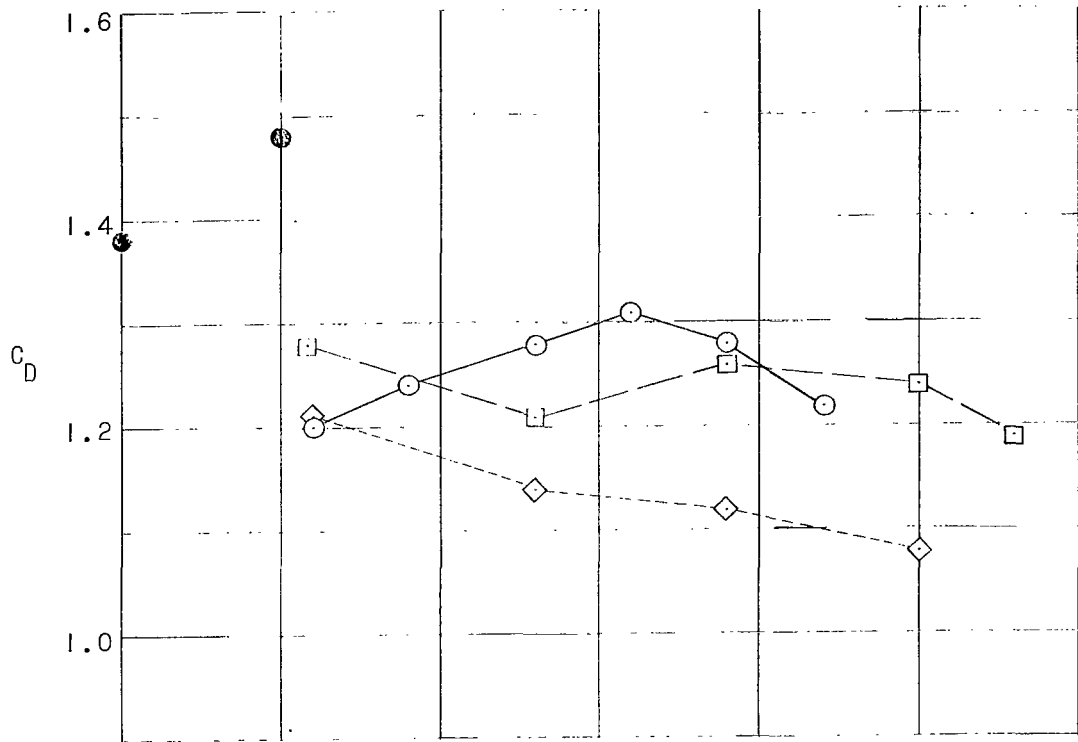
Figure 8.- Effect of corner radius on C_D and Δ for toroid-membrane models. $L_3 = 0$; $L_{cg}/r_b = 0.6$ to 0.9; $l/d = 10$.
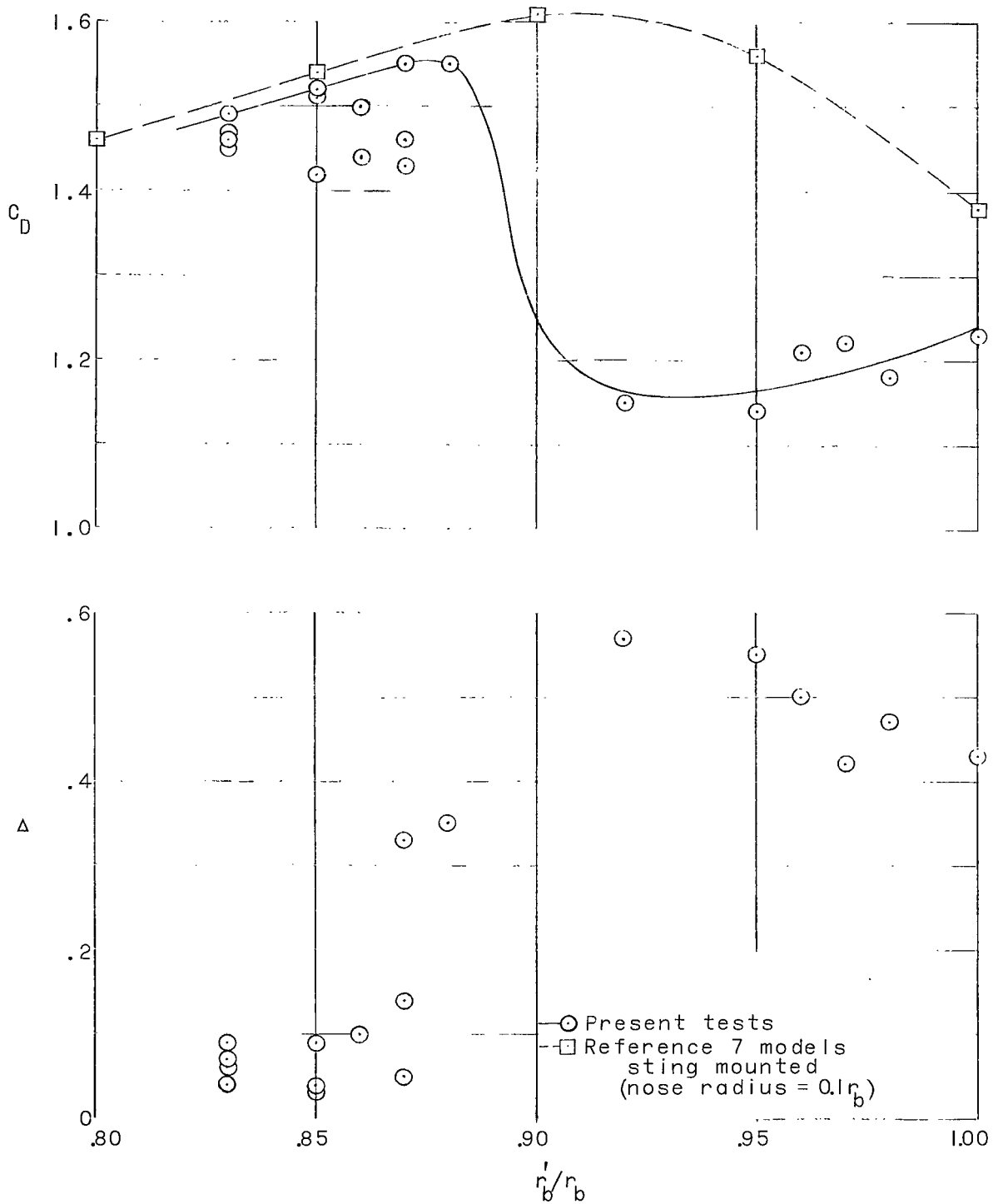
Figure 9.- Effect of reduced base on C_D and Δ for toroid-membrane models. $t_b/r_b = 0.01$ to 0.08; $l/d = 8$.
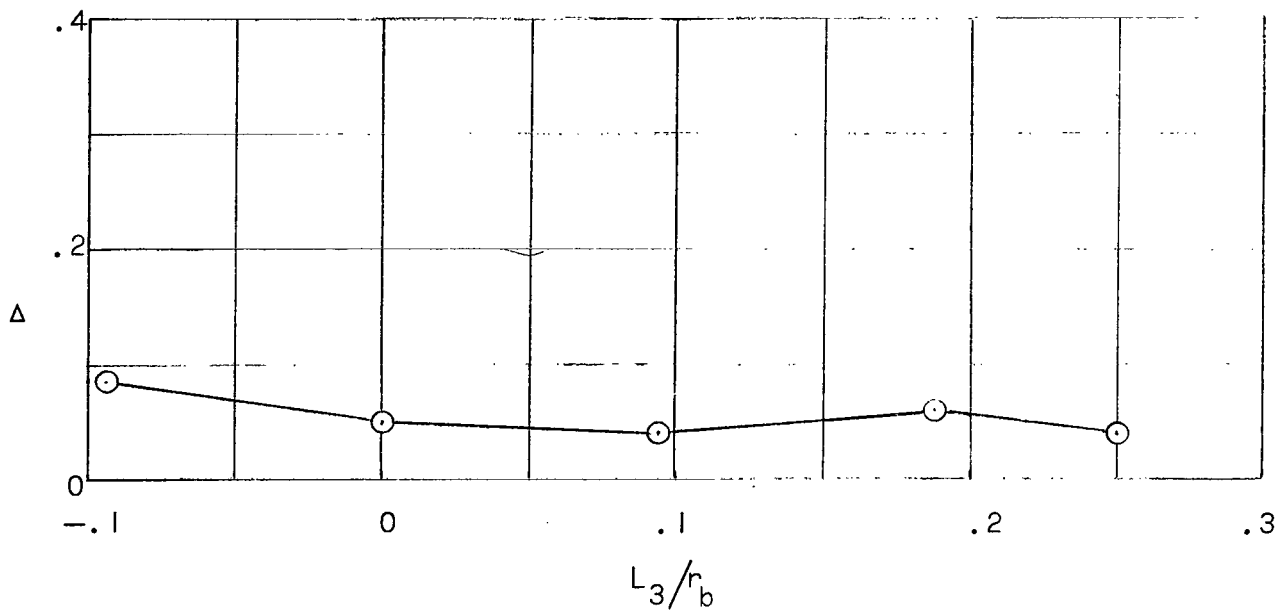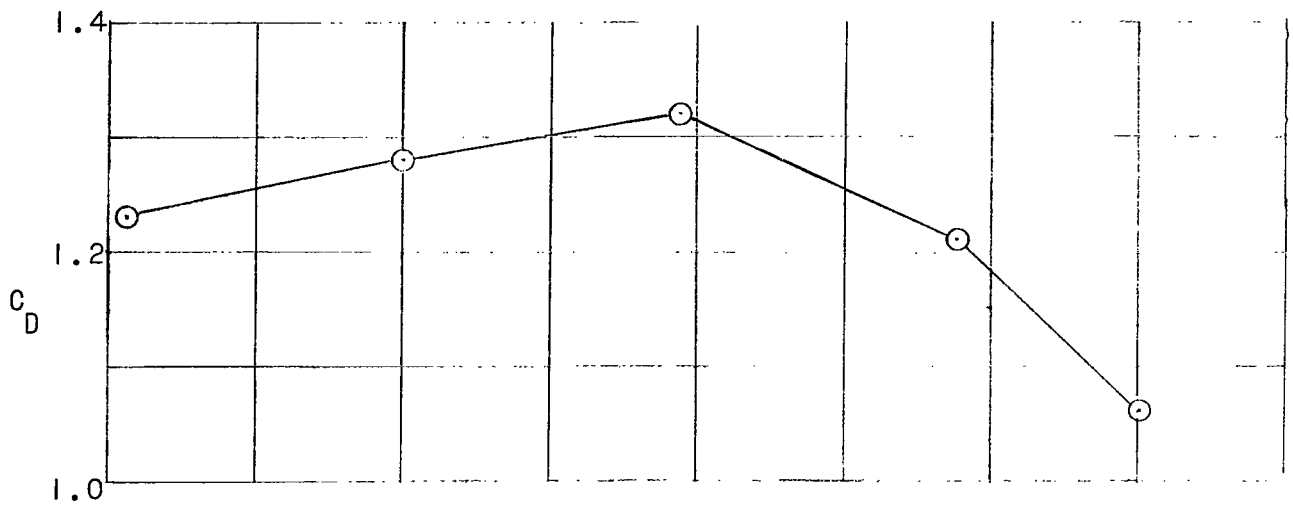
Figure 10.- Effect of pivot location on C_D and Δ for toroid-membrane models. $\Phi = 5^0$; $r_c/r_b = 0.06$; $L_b/r_b = 0.25$; $l/d = 10$.
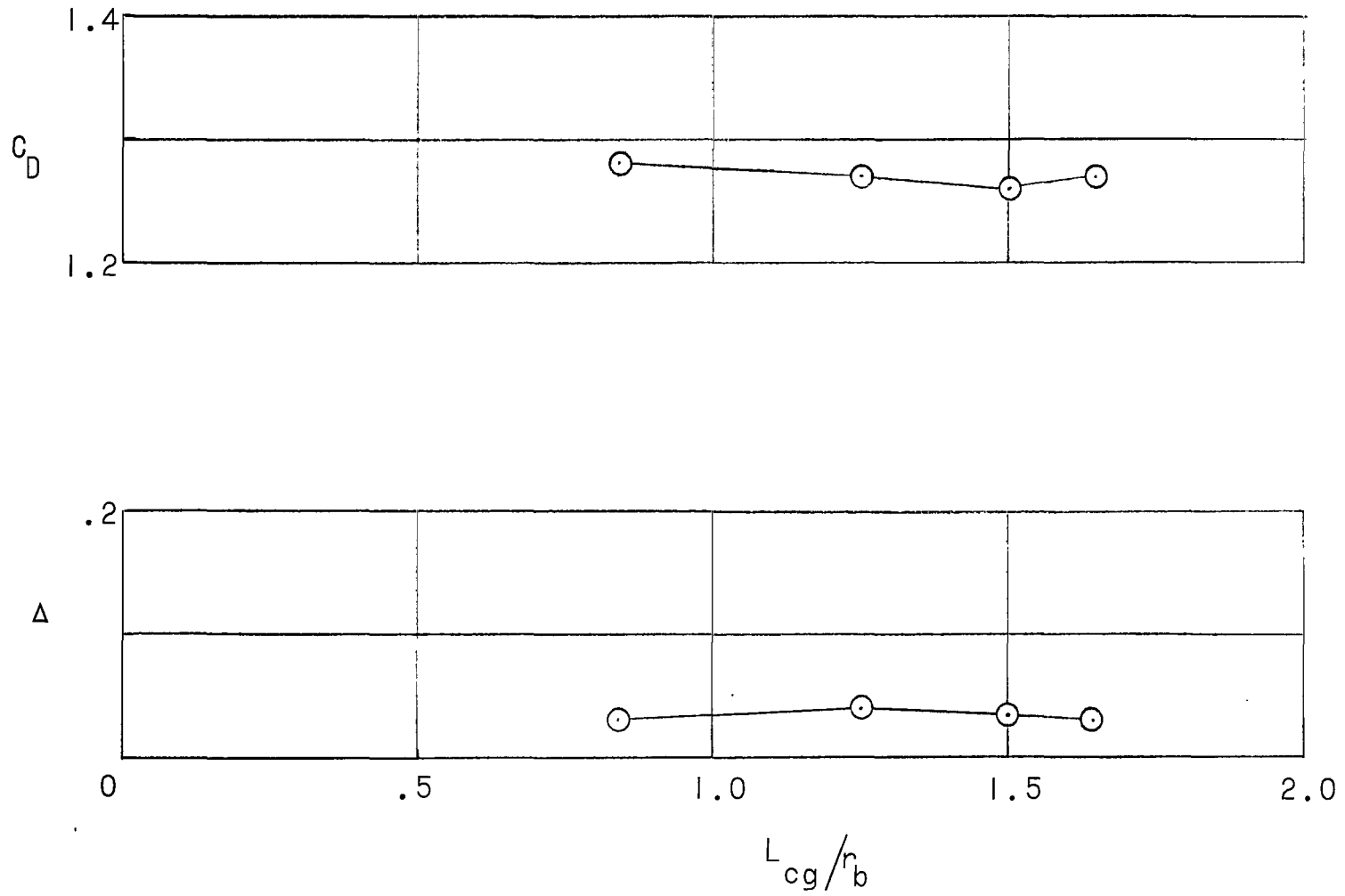
Figure 11.- Effect of center-of-gravity location on C_D and Δ for toroid-membrane models with toroidal ring. $r_c/r_b = 0.19$; $L_b = 0$; $l/d = 10$.
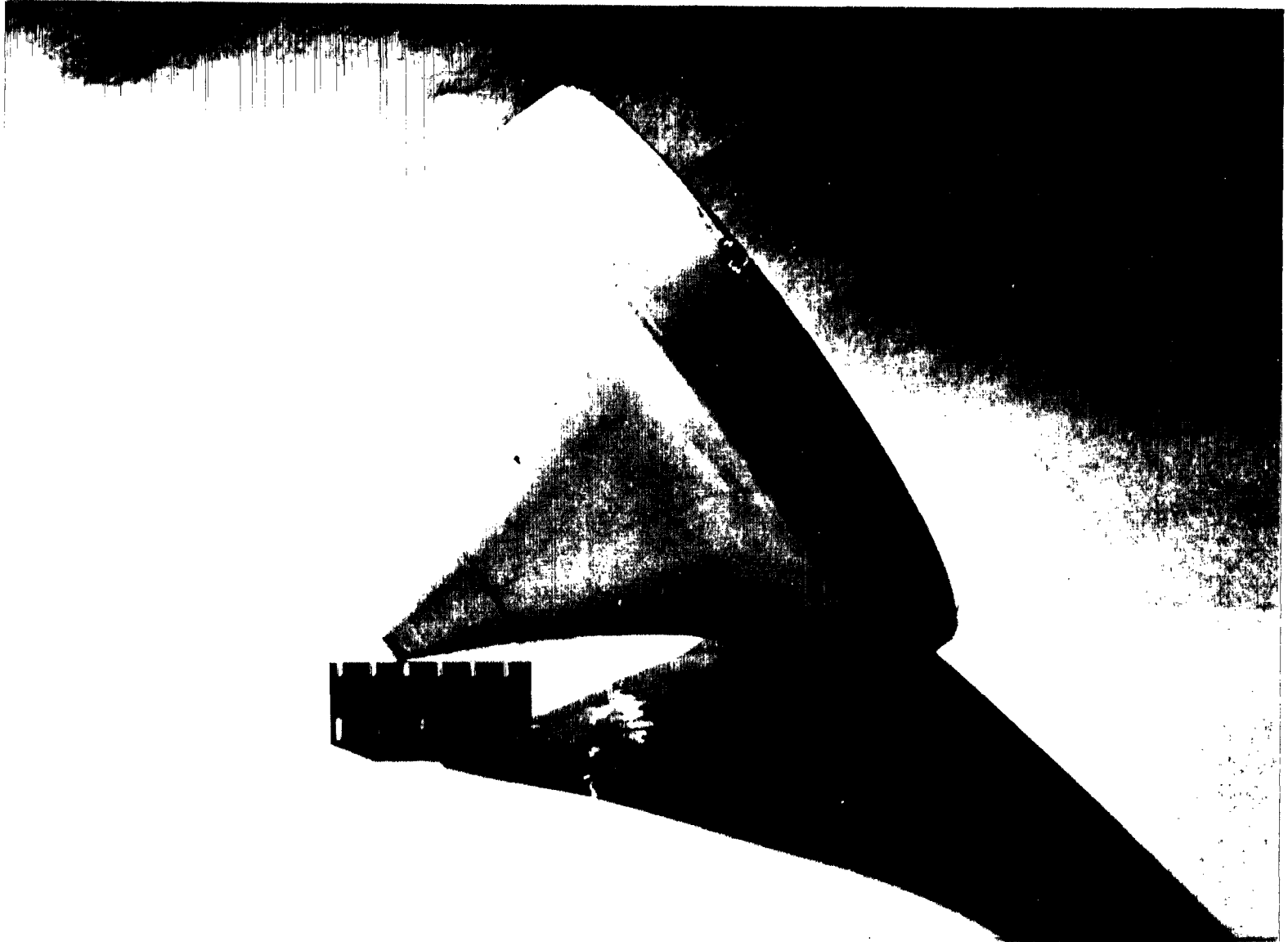
Figure 12.- Flexible toroid-membrane model. (Model 45.)
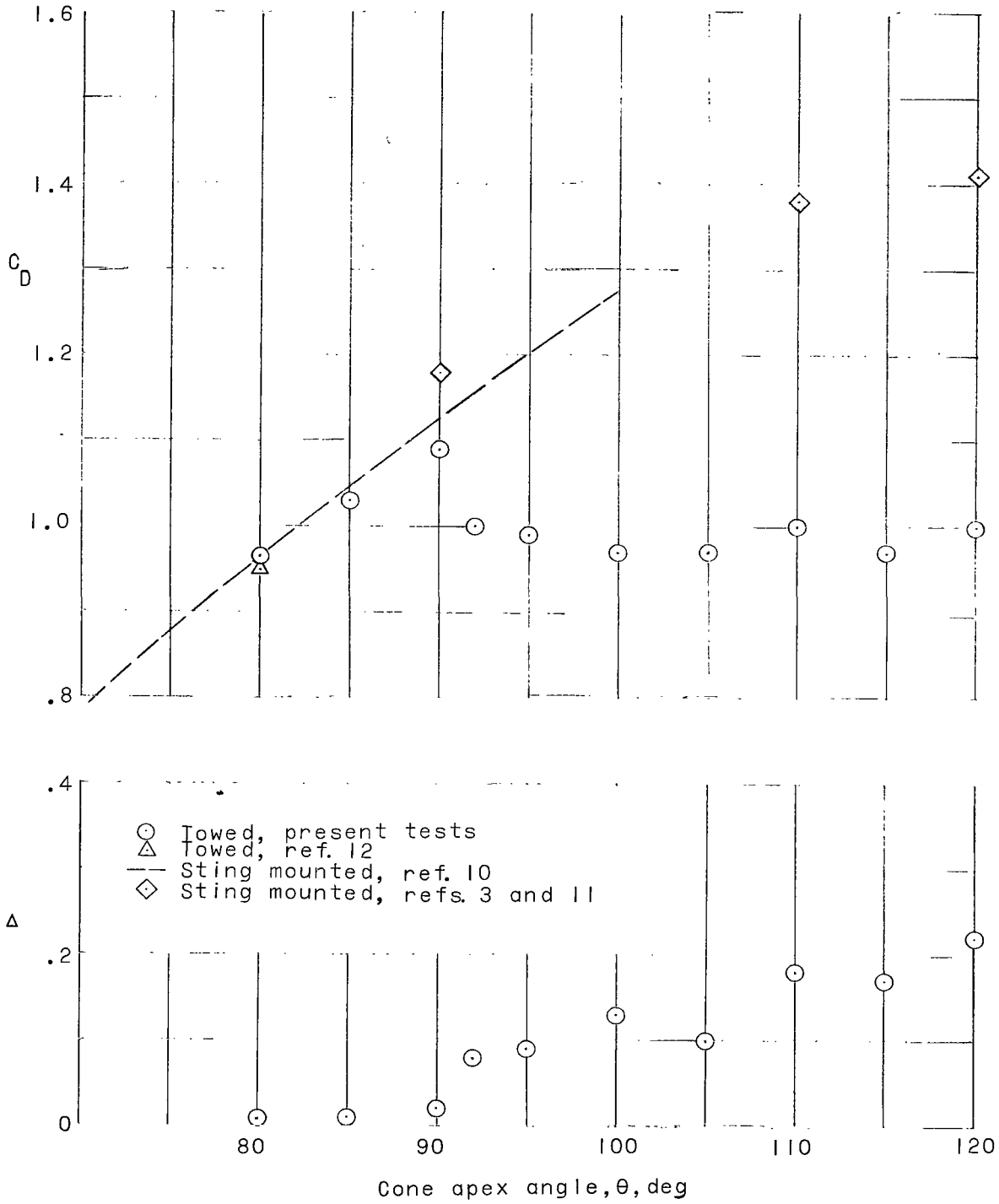
Figure 13.- Experimental variation of C_D and Δ with cone angle at Mach 3. l/d = 8 to 10 for towed cones.
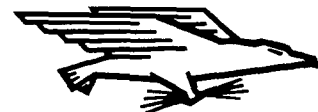
03U 001 26 51 30S   70119   00903
AIR FORCE WEAPONS LABORATORY /WLOL/
KIRTLAND AFB, NEW MEXICO 87117

ATT E. LOU BOWMAN, CHIEF,TECH. LIBRARY

*"The aeronautical and space activities of the United States shall be
conducted so as to contribute . . . to the expansion of human knowl-
edge of phenomena in the atmosphere and space. The Administration
shall provide for the widest practicable and appropriate dissemination
of information concerning its activities and the results thereof."*

— NATIONAL AERONAUTICS AND SPACE ACT OF 1958

NASA 'SCIENTIFIC AND TECHNICAL PUBLICATIONS

TECHNICAL REPORTS: Scientific and
technical information considered important,
complete, and a lasting contribution to existing
knowledge.

TECHNICAL NOTES: Information less broad
in scope but nevertheless of importance as a
contribution to existing knowledge.

TECHNICAL MEMORANDUMS:
Information receiving limited distribution
because of preliminary data, security classifica-
tion, or other reasons.

CONTRACTOR REPORTS: Scientific and
technical information generated under a NASA
contract or grant and considered an important
contribution to existing knowledge.

TECHNICAL TRANSLATIONS: Information
published in a foreign language considered
to merit NASA distribution in English.

SPECIAL PUBLICATIONS: Information
derived from or of value to NASA activities.
Publications include conference proceedings,
monographs, data compilations, handbooks,
sourcebooks, and special bibliographies.

TECHNOLOGY UTILIZATION
PUBLICATIONS: Information on technology
used by NASA that may be of particular
interest in commercial and other non-aerospace
applications. Publications include Tech Briefs,
Technology Utilization Reports and Notes,
and Technology Surveys.

Details on the availability of these publications may be obtained from:

SCIENTIFIC AND TECHNICAL INFORMATION DIVISION

NATIONAL AERONAUTICS AND SPACE ADMINISTRATION
Washington, D.C. 20546